

Smart Phone Robot Made of Smart Soft Composite (SSC)

Wei Wang*, Hugo Rodrigue*, Jang-Yeob Lee*, Min-Woo Han*, Sung-Hoon Ahn***†

ABSTRACT: Soft morphing robotics making use of smart material and based on biomimetic principles are capable of continuous locomotion in harmony with its environment. Since these robots do not use traditional mechanical components, they can be built to be light weight and capable of a diverse range of locomotion. This paper illustrates a flexible smart phone robot made of smart soft composite (SSC) with inchworm-like locomotion capable of two-way linear motion. Since rigid components are embedded within the robot, bending actuators with embedded rigid segments were investigated in order to obtain the maximum bending curvature. To verify the results, a simple mechanical model of this actuator was built and compared with experimental data. After that, the flexible robot was implemented as part of a smart phone robot where the rigid components of the phone were embedded within the matrix. Then, experiments were conducted to test the smart phone robot actuation force under different deflections to verify its load carrying capability. After that, the communication between the smart phone and robot controller was implemented and a corresponding phone application was developed. The locomotion of the smart phone robot actuated through an independent controller was also tested.

Key Words: Smart phone robot, Shape memory alloy, Smart soft composite, Inchworm-like locomotion

1. INTRODUCTION

There is growing interest in developing smart structures utilizing smart materials or new mechanisms to fulfill increasingly diverse and specific objectives and tasks. Recently smart electronics taking many shapes and fulfilling diverse functions have been commercialized such as wearable electronics. Smart structures capable of integrating diverse functions into a single structure have drawn much attention. There exist different types of smart materials, such as shape memory alloy (SMA), shape memory polymers (SMPs), electro-active polymers (EAPs), ionic polymer metal composite (IPMC), lead zirconium titanate (PZT). Amongst these, SMA composite actuators can provide large deformations and are well suited for bio-inspired applications [1]. These actuators use joule heating to recover an applied mechanical pre-strain of the SMA material, which is used to induce a large deformation of the host matrix. Therefore, these actuators are flexible, can bend through their entire length and capable of large deflections [2]. The properties of the host matrix have a strong influence on

the behavior of the actuator. A micro robot fish with caudal biomimetic fin was built utilizing a SMA composite actuator by Wang *et al.* [3]. Ahn *et al.* proposed a smart soft composite (SSC) structure with embedded soft anisotropic material in order to achieve complex bending and twisting deformation [4]. Using this type of structure, a turtle-like swimming robot using a smart soft composite (SSC) structure was fabricated by Kim *et al.* [5].

This study follows our previous research [6,7] of an inchworm-inspired robot. In this study, a soft morphing smart phone robot was designed and fabricated that is both lightweight and thin. This robot is capable of large-stride two-way linear motion. The main structure of this robot is a flexible actuator with embedded rigid segment which was investigated first to gain a better understanding of how to obtain maximum bending curvature even with rigid body segments. Then the actuator was applied in the shape of an inchworm robot with integrated rigid electronic parts of a smart phone in order to obtain a robot capable of automatic identification, judgment and execution. An application developed for the Android

Received 7 January 2015, received in revised form 21 April 2015, accepted 27 April 2015

*Department of Mechanical and Aerospace Engineering, Seoul National University

†Institute of Advanced Machinery and Design, Seoul National University

***†Corresponding author (E-mail: ahnsh@snu.ac.kr)

operating system was enabled to guide the locomotion of the robot through Bluetooth communication.

2. SOFT ACTUATOR WITH RIGID SEGMENT

The entire structure of the smart phone robot is an SMA wire-based flexible actuator with the embedded rigid segments of the smart phone. In order to gain a better understanding of how to obtain maximum bending curvature even with rigid body segments, an experiment was conducted to investigate the effect of rigid segments on the maximum bending deformation [8]. Using these results, a simple mechanical model was built.

2.1 Experiments

The configuration of the actuator is shown in Fig. 1 where the specimen is comprised of three segments: the flexible segment with a length of L_f , two rigid segment in blue with a total length of L_r and the total length of the actuator is denoted as L . A set of actuators were built to verify the maximum in-plane bending curvatures depending of the ratio of the length of the flexible segment versus the total length. The fabrication process is similar to that of the robot described in [7]. All the specimens have dimensions of $80 \times 10 \times 3$ (mm, $L \times W \times T$), but with different ratios of flexible segment length to total length, defined as μ :

$$\mu = L_f / (L_r + L_f) \quad (1)$$

An SMA wire was placed eccentrically from the middle plane with a distance d of 0.75 mm. Ten types of specimens were fabricated with different ratios of μ corresponding to 1/7, 1/6, 1/5, 1/4, 1/3, 2/5, 1/2, 6/10, 7/10, and 4/5. Three samples were tested for each configuration and all were tested with an electric current of 1.0 A as the initial input current and actuated until no more visible deformation occurred. The final shape was then used to measure the maximum bending angle θ . Then the corresponding radius of curvature, R , was calculated using (2) and the mean value of the results are shown in Table 2.

$$R = 180 L_f / (\pi\theta) \quad (2)$$

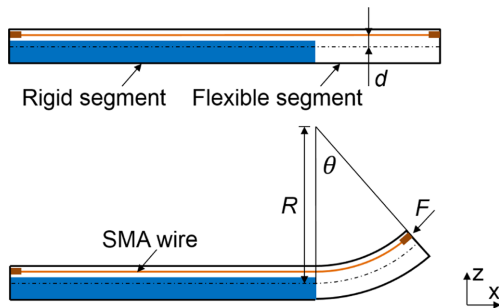


Fig. 1. Bi-dimensional model of soft actuator with initial position and bending status

2.2 Mechanical Model

A mechanical model was developed for the configuration shown in Fig. 1. The bending deformation of the actuators induced by the moment produced by the contraction of the SMA wire is shown in this figure and can be calculated as:

$$M = Fd = \sigma A_{\text{SMA}} d \quad (3)$$

where F is the contraction force generated by the SMA wire, A_{SMA} is the area of the cross-section of the SMA and σ is the stress generated by the SMA wire. The constitutive law of the SMA austenite transformation under the assumption of zero initial stress, a negligible thermoelastic term and complete austenite transformation [1] is calculated using:

$$\sigma = E_a \varepsilon_{\text{cur}} \quad (4)$$

where E_a is the Young's modulus of an SMA wire in austenite phase and ε_{cur} is the SMA wire strain in situ. Throughout the bending process, the SMA wire strain becomes getting shorter, and the shortened value is expressed as $\varepsilon_s = \varepsilon_{\text{int}} - \varepsilon_{\text{cur}}$ where ε_{int} is the initial strain. Considering the initial length of SMA wire was equal to the length of model, the bending angle of the circumference is given as:

$$\theta = L_f / R = (L_f - \varepsilon_s L) / (R - d) \quad (5)$$

Using (1)~(5) and by applying Euler's beam theory:

$$d\theta/ds = 1/R = M/EI \quad (6)$$

where EI is the equivalent bending stiffness of the model, the maximum bending radius is obtained as:

$$R = (\mu E_a A_{\text{SMA}} d^2 + EI) / (E_a A_{\text{SMA}} d \varepsilon_{\text{int}}) \quad (7)$$

The material properties of the PDMS and the SMA wires are listed in Table 1. The experimental results and the results obtained from the model are listed in Table 2.

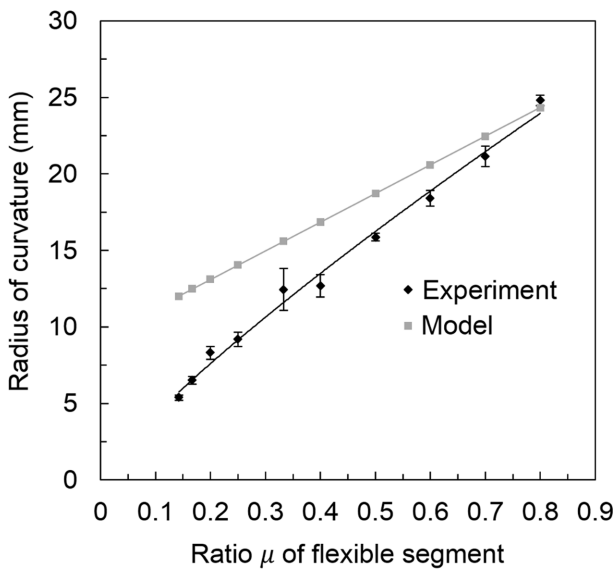
From the results, it is easy to see that for a lower μ , the minimum bending radius decreases significantly. It can be seen that a reduction in bendable section for the actuator leads to increased bending in this section. Fig. 2 shows a comparison

Table 1. Material properties

Material properties	Value (unit)
SMA martensite start temperature	$M_s = 52^\circ\text{C}$
SMA martensite finish temperature	$M_f = 42^\circ\text{C}$
SMA austenite start temperature	$A_s = 68^\circ\text{C}$
SMA austenite finish temperature	$A_f = 78^\circ\text{C}$
SMA martensite Young modulus	$E_m = 28 \text{ GPa}$
SMA austenite Young modulus	$E_a = 75 \text{ GPa}$
PDMS Young modulus (25°C)	$E_{\text{PDMS}} = 1.8 \text{ MPa}$
SMA initial strain	$\varepsilon_{\text{int}} = 5\%$
SMA diameter	$d_{\text{SMA}} = 0.203 \text{ mm}$

Table 2. Maximum bending radius of curvature from experiments and model

Ratio μ	Experiment (mm)	Model (mm)
1/7	5.38	12.02
1/6	6.52	12.47
1/5	8.30	13.09
1/4	9.19	14.03
1/3	12.45	15.59
2/5	12.68	16.84
1/2	15.88	18.72
3/5	18.42	20.59
7/10	21.14	22.47
4/5	24.80	24.34

**Fig. 2.** Variation tendency of maximum bending radius of curvature experiments and mechanical model

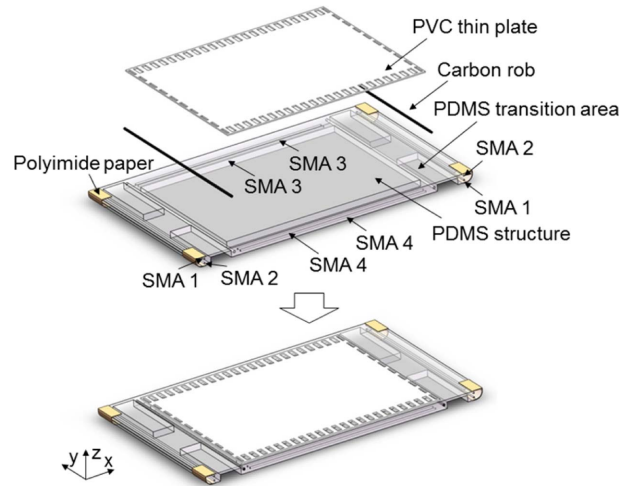
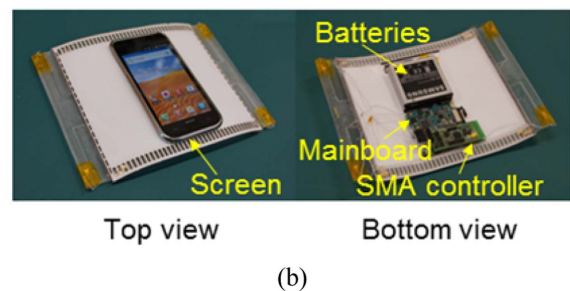
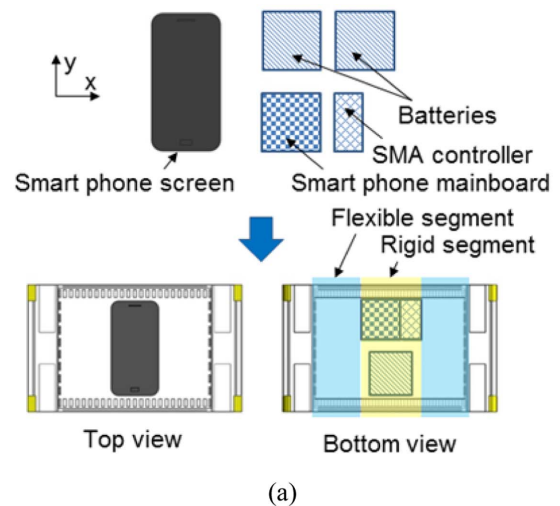
of the results from the model with that of the experiments. As shown in the figure, the results from the experiment show a higher response to a reduction in length of the bending section compared to the model. This is possibly due to the SMA wire not following the change of arc of curvature of the matrix by deforming the matrix to follow a more direct path, which would increase the actuation moment.

3. APPLICATION TO SMART PHONE ROBOT

3.1 Smart Phone Robot Architecture

SMA wires were used as the active components and were embedded in the matrix eccentrically to obtain a large bending deformation. The robot structure was designed as a thin rectangular shape with a structure size of $196 \times 140 \times 4$ (mm, $L \times W \times T$). Fig. 3 shows the detailed design of the overall structure. In this figure, the SMA wires with the same number are to be connected in series such that they are simultaneously

actuated. There are total four group SMA wires: SMA 1 and SMA 2 are used to actuate each of the feet and SMA 3 and SMA 4 are used to actuate each side of the body. The feet of the robot were segmented in sections with different coefficient of friction with two ends being covered by polyimide tape to reduce the coefficient of friction. The PVC plate, with a thickness of 0.4 mm, is used to reduce the weight of the overall structure, to enhance the stability and to obtain a larger and

**Fig. 3.** Overall robot structure and its components**Fig. 4.** (a) All components and CAD model of integrated smart phone robot. (b) Fabricated smart phone robot

faster recovery stroke of the structure. The carbon rods are used to maintain the intended shape of the matrix during linear and turning locomotion of the robot. The PDMS has a transition area with a thickness of 1 mm between the feet and the body to decouple the deformation of the body and the feet.

In order to design and build a smart phone robot capable of a high-level of interaction with humans are capable of being used in surveillance and communication, a smart phone (Samsung Galaxy SHW-M110S) was integrated with the crawling robot introduced previously. The smart phone is comprised of three main functional parts including the screen, main board and battery. The batteries' voltage required to actuate the SMA wires and to run the smart phone is 7.4 V and 3.7 V respectively. Therefore, two batteries with a voltage of 3.7 V were used. The position of the components within the structure is shown in Fig. 4. The electronics placed in the middle of the body are rigid and prevent deformation in this section. As predicted by the previous experiment in Section 2, it was observed that the radius of curvature of the bending flexible parts was reduced. Although the middle section cannot bend, the bending deformation of the soft section is increased.

3.2 Actuation Force Evaluation

The smart phone robot should have a good load-carrying capacity considering it must carry the weight of the embedded electronics weighing nearly 150 gram. To measure the capability of the robot, a jig preventing motion of the middle section of body was built and is shown in Fig. 5. The actuating force of the smart phone robot was measured using a dynamometer (Kistler type 9256C2). The experiment was conducted for tip deflections varying from 8 mm to 35 mm by adjusting the height of the jig in increments of 3 mm, under an initial current of 1.0 A for 20 seconds. A smooth acrylic plate is used to negate the impact of the friction on the surface of the force sensor. The detailed experimental setup is shown in Fig. 5. The middle part of the robot structure is fixed with a jig and its position is adjusted by a using three-dimensional platform.

When actuating the SMA wires embedded in the robot, the force generated by one of the feet along the vertical direction is measured and plotted in Fig. 6. The results show that the actuation force drops almost linearly with the increase in tip deflection. However, for deflections ranging from 18 mm to

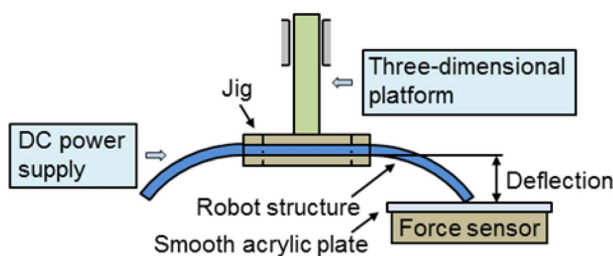


Fig. 5. Actuation force experimental setup

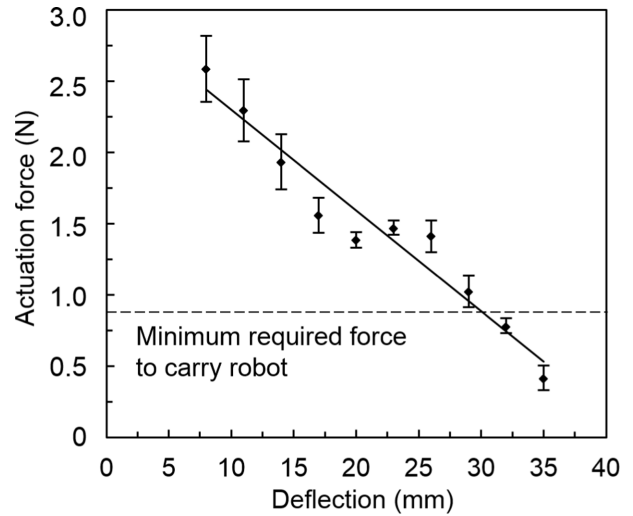


Fig. 6. Experimental results of actuation force

26 mm the actuation force is nearly constant. The weight of the smart phone robot is 182.5 gram, which is equivalent to 1.78 N, so each foot should be able to carry a load of 0.89 N. As shown in Fig. 6, the largest deformation able to carry this is of nearly 30 mm.

3.3 Application Development

A custom PCB installed with an ATmega8 microcontroller and Bluetooth module was used to realize communication between the smartphone's interface and the SMA wire controller. To realize the communication between the cell phone and the robot controller, an application built by App Inventor using a graphical interface was developed. The communication was established between the Bluetooth modules of the cell phone and the robot controller. The application is capable of sending commands for moving forward, backward, turning

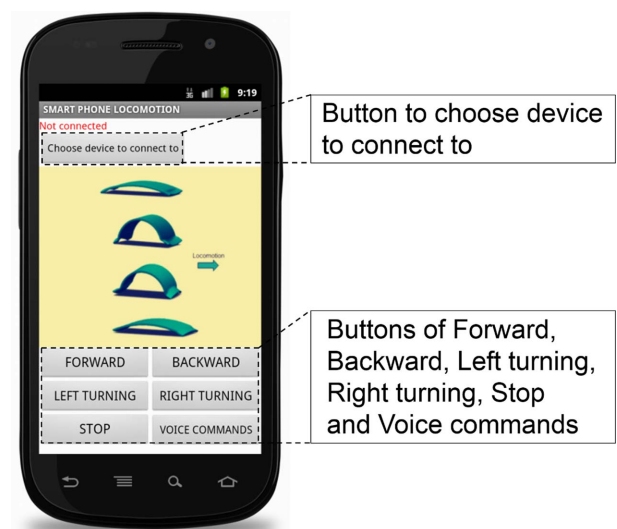


Fig. 7. Interface of phone app for smart phone robot locomotion

left, right and to stop either by pressing buttons on the screen or through voice command. The interface of this application is shown in Fig. 7.

3.4 Smart Phone Robot Locomotion

The experiments were conducted on a flat horizontal desk at room temperature. The currents was determined to be 0.55 A and 1.0 A to actuated the SMA wires in the feet and the body. A digital camera is used to record the locomotion of the robot. The SMA wires actuated throughout one stride using a square wave pattern is shown in Fig. 8. The SMA controller has four digital outputs that direct current to the four groups of SMA wires using the 7.4 V batteries connected in series. The robot completes a stride in 20 seconds and needs a waiting period of 5 seconds between each stride for a total cycle time of 25 seconds, as shown in Fig. 8. The locomotion the of smartphone robot was evaluated for five strides totaling 125 seconds with a total displacement of nearly 75 mm. The results show that the average stride length is 15 mm and the corresponding average speed is 0.6 mm/s. The linear motion for one stride is shown in Fig. 9.

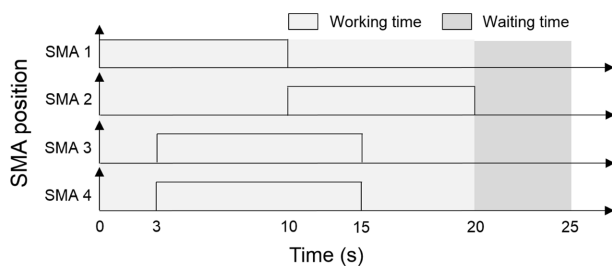


Fig. 8. Current patterns for locomotion of smart phone robot

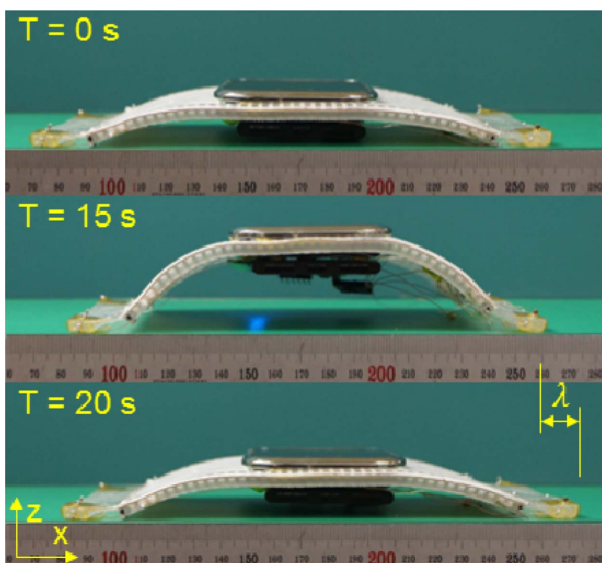


Fig. 9. Linear motion of smart phone robot

4. CONCLUSIONS

In this research, experiments were carried to evaluate the bending performance of a flexible actuator with embedding rigid segments which showed that the length of the rigid segments reduces significantly the radius of curvature of the actuator. Then, a smart phone robot based on the inchworm-like robot was built which incorporates rigid electronic components. The actuation force of the robot structure was tested at different heights of actuation which showed that the actuation force reduced linearly with the actuation height.

Afterwards, Bluetooth communication between the smart phone robot and an SMA controller was realized through an Android application which allowed the user to command the robot manually or through voice recognition. This kind of robot capable of bidirectional communication has the potential of being used in rescue and reconnaissance situations where humans or larger robots are not capable of access.

Future work is required to improve the efficiency of the robot motion and to reduce its energy consumption. In addition, efforts will be made to integrate flexible components rather than stiff ones in order to build an entirely soft robot capable of complex locomotion and advanced communication capabilities. Furthermore, artificial intelligence will be investigated for the robot to be capable of independent decision making; of automatic identification, judgment and execution utilizing different structure mechanisms, sensors, applications and more diverse means of communication.

ACKNOWLEDGEMENT

This work was supported by the Industrial Strategic technology development program (10049258) funded by the Ministry of Knowledge Economy (MKE, Korea) and the National Research Foundation of Korea (NRF) grant funded by the Korea government (MEST) (No. NRF-2010-0029227). The deepest gratitude is expressed to the providence of God.

REFERENCES

- Smith, C., Villanueva, A., Joshi, K., Tadesse, Y., and Priya, S., "Working Principle of Bio-inspired Shape Memory Alloy Composite Actuators," *Smart Materials and Structures*, Vol. 20, No. 1, 2011, pp. 012001.
- Rodrigue, H., Wang, W., Bhandari, B., Han, M.W., and Ahn, S.H., "Cross-shaped Twisting Structure Using SMA-based Smart Soft Composite", *International Journal of Precision Engineering and Manufacturing-Green Technology*, Vol. 1, No. 2, 2014, pp. 153-156.
- Wang, Z., Hang, G., Wang, Y., Li, J., and Du, W., "Embedded SMA Wire Actuated Biomimetic Fin: A Module for Biomimetic Under Water Propulsion", *Smart Materials and Structures*, Vol. 17, No. 2, 2008, pp. 025039.

4. Ahn, S.H., Lee, K.T., Kim, H.J., Wu, R., Kim, J.S., and Song, S.H., "Smart Soft Composite: An Integrated 3D Soft Morphing Structure using Bend-twist Coupling of Anisotropic Materials", *International Journal of Precision Engineering and Manufacturing*, Vol. 13, No. 4, 2012, pp. 631-634.
5. Kim, H.J., Song, S.H., and Ahn, S.H., "A Turtle-like Swimming Robot using a Smart Soft Composite (SSC) Structure", *Smart Materials and Structures*, Vol. 22, No. 1, 2013, pp. 014007.
6. Wang, W., Lee, J.Y., Kim, J.S., Lee, K.T., Kim, H.S., and Ahn, S.H., "Locomotion of Crawling Robots Made of Smart Soft Composite (SSC)", *2013 Proceeding of the 13th International Conference on Control, Automation and Systems (ICCAS)*, Gwangju, Korea, Oct. 2013, pp. 309-312.
7. Wang, W., Lee, J.Y., Rodrigue, H., Song, S.H., Chu, W.S., and Ahn, S.H., "Locomotion of Inchworm-inspired Robot Made of Smart Soft Composite (SSC)", *Bioinspiration & Biomimetics*, Vol. 9, No. 4, 2014, pp. 046006.
8. Wang, W., Rodrigue, H., Chu, W.S., Song, S.H., and Ahn, S.H., "SMA-Based Soft Morphing Actuators with Flexible and Rigid Segments", *Korean Society for Precision Engineering, Autumn Conference*, 2013, pp. 1079-1080.